

Quantitative Measurement of Focused Ultrasound Pressure Field by Background-subtracted Shadowgraph Using Holographic Diffuser as Screen

散乱スクリーンを用いた差分シャドウグラフ法における集束超音波音場の定量化

Ryo Miyasaka[‡], Jun Yasuda, Mohd Syahid, Shin Yoshizawa, and Shin-ichiro Umemura (Tohoku Univ.)

宮坂 遼[‡], 安田 惇, Mohd Syahid, 吉澤 晋, 梅村 晋一郎 (東北大学)

1. Introduction

Accurate measurement of ultrasound field is important to ensure and improve the safety and efficacy of the medical use of ultrasound such as HIFU (High Intensity Focused Ultrasound) treatment. In contrast to the mechanically scanned hydrophone, the optical method takes very short time, and does not disturb the acoustic field.

We successfully reconstructed a pressure field by applying a computed tomography (CT) algorithm to the background-subtracted shadowgraphs^[1-3], for the accuracy of which the optical propagation length between the ultrasound field and the optical imaging plane is important. In this study, we improve it by using a holographic diffuser as the imaging screen.

2. Method

The spatial change of water density due to acoustic pressure, distort the incident planar optical wavefront to a wavy one. The light at this moment is considered to have received only phase modulation without intensity modulation. The phase variation modulates the optical intensity during propagation and forms the shadowgraph image. **Fig. 1** shows the optical intensity modulation in a shadowgraph^[3]. Assuming the optical refraction angle θ_y due to the ultrasound pressure distribution is sufficiently small, the relation between optical intensity and acoustic pressure can be shown as follows.

$$\frac{I_{on} - I_{off}}{I_{on}} = -l \frac{\partial n}{\partial p} \left(\frac{\partial^2}{\partial x^2} + \frac{\partial^2}{\partial y^2} \right) \int p dz \quad (1)$$

Here, the geometrical optics approximation was applied. I_{on} and I_{off} are the optical intensities on the imaging plane with and without ultrasound exposure, respectively. The piezo-optic coefficient^[4], $\partial n / \partial p$ for water is calculated to be $1.32 \times 10^{-10} \text{ Pa}^{-1}$ from its density of 10^3 kg/m^3 , sound speed of 1500 m/s , refractive index of 1.34 at $20 \text{ }^\circ\text{C}$, and the

optical wavelength of 589 nm . To define the optical propagation length l in eq. (1) precisely, we used a holographic diffuser as the imaging screen.

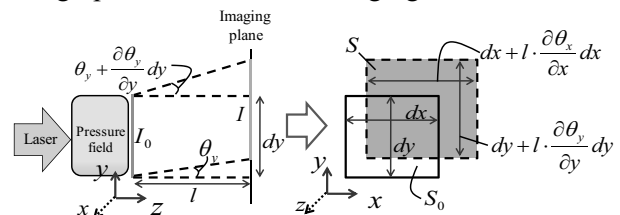


Fig. 1 Intensity modulation due to phase variation.

3. Experiment

Fig. 2 shows the optical measurement setup for the modified shadowgraph. The pulsed laser (CryLas FDSS 532-Q2, wavelength: 532 nm , pulse length: not more than 1.3 ns , power: 4 kW) was expanded by a convex lens (diameter: 3 mm , focal length: 3 mm) and collimated by a lens (diameter: 150 mm , focal length: 1500 mm) in front of the water tank. Furthermore, the laser passing through the ultrasound field was converged by a lens behind the water tank. We measured the optical depth of field and set a holographic diffuser (Optical Solutions, transmittance: above 90% , diffuse angle: 5 degree) there as the imaging screen. Here, its scattering amplification is different at each point. For this reason, we moved a holographic diffuser slightly up and down in capturing many images and averaged them. The shadowgraph images were taken by a CCD camera (Sony XCD-U100, $1200 \times 1600 \text{ pixel}$). The laser pulse and the ultrasound from the transducer were synchronized by a function generator (NF WF 1974) exciter every 1 ms , and the shutter speed of the CCD camera was 1 ms . A lead zirconate titanate (PZT) transducer (aperture and diameter: 70 mm , center frequency: 1.14 MHz) was used to generate the ultrasound pressure field to be reconstructed. 50 images were acquired and averaged. 3D ultrasound pressure field was reconstructed by applying a CT algorithm

ryo-m@ecei.tohoku.ac.jp

considering that the pressure field had cylindrical symmetry.

We compared the reconstruction from optical measurement and the measurement by a membrane hydrophone with an active diameter of 200 μm . The hydrophone was scanned every 400 μm on the axis.

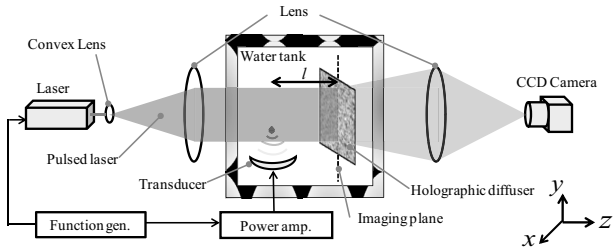


Fig. 2 Optical measurement setup.

4. Results and discussion

Fig. 3 (a) and (b) show the acoustic pressure on the axial direction (x axis) and the lateral direction (y axis) obtained with a small holographic diffuser at a short optical propagation length $l=40$ mm. The peak pressure was 4.5 MPa_{pp} . In **Fig. 3 (a)**, the outline of the main lobe from hydrophone agreed well with the optical measurement. In **Fig. 3 (b)**, good overall agreement is seen along the lateral direction.

For a higher S/N ratio at the side lobes, a longer propagation length $l=200$ mm was chosen and the result is shown in **Fig. 4**. Here, the amplitude was normalized based on the absolute peak pressure in **Fig. 3 (a)**. The side lobes agree well, but the reconstruction seems to have failed in the main lobe probably because the assumption for eq. (1) started failing.

Then, we used the combination of the two sets of experimental data with optical propagation lengths of 40 and 200 mm for the main lobe and side lobes, respectively. The pressure on the axial direction reconstructed from the combined data is shown in **Fig. 5**. Good agreement can be seen for both main and side lobes. In this way, we can measure the pressure field up to 4.5 MPa_{pp} .

In comparison to hydrophone, the absolute pressure from the optical measurement was about 50 %. Although absolute measurement should be possible by the proposed method in principle, calibration is still needed at this stage.

5. Conclusions

We reconstructed an ultrasound pressure field from background-subtracted shadowgraphs. Using a holographic diffuser, we were able to define the optical propagation length precisely. Using two sets of shadowgraphs with optimal optical propagation

lengths, we successfully obtained ultrasound pressure field identical to hydrophone measurement up to 4.5 MPa_{pp} . The use of even shorter optical propagation length should be studied for higher acoustic pressure levels as used on HIFU. This will also be discussed in the presentation.

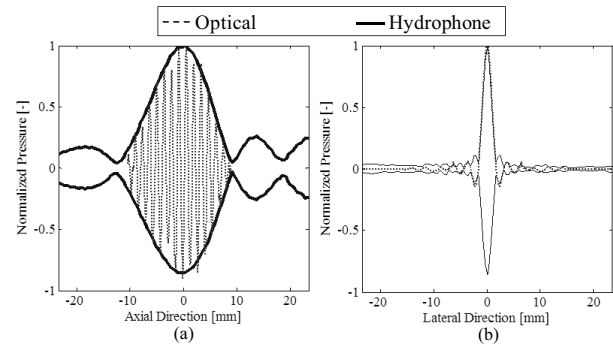


Fig. 3 Comparison between two methods for $l=40$ mm. (a) axial direction, (b) lateral direction.

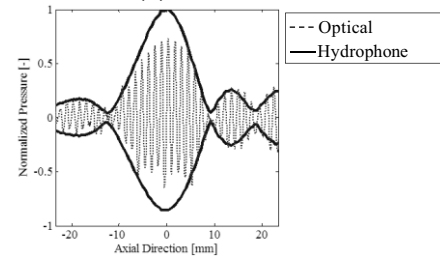


Fig. 4 Comparison between two methods for $l=200$ mm.

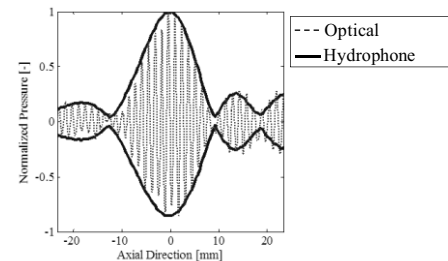


Fig. 5 Comparison between two methods for the combined data.

Acknowledgment

This work was supported by a Grant-in-Aid for Scientific Research from the Japan Society for the Promotion of Science (JSPS)

References

1. T. A. Pitts and J. F. Greenleaf: J. Acoust. Soc. Am. **108**, 2873 (2000).
2. H. Ouchi, N. Kudo, K. Yamamoto, and H. Sekimizu: IEICE Tech. Rep. **19**, 9 (2004). [in Japanese]
3. R. Omura, Y. Shimazaki, S. Yoshizawa and S. Umemura: Jpn. J. Appl. Phys. **50**, 07HC07 (2011).
4. M. J. Crocker: Encycl. Acoust. **1** (1997) 1